LETTER

doi:10.1038/nature10177

In vivo genome editing restores haemostasis in a mouse model of haemophilia

Hojun Li[1], Virginia Haurigot[1], Yannick Doyon[2], Tianjian Li[2], Sunnie Y. Wong[2], Anand S. Bhagwat[1], Nirav Malani[3], Xavier M. Anguela[1], Rajiv Sharma[1], Lacramiora Ivanciu[1], Samuel L. Murphy[1], Jonathan D. Finn[1], Fayaz R. Khazi[1], Shangzhen Zhou[1], David E. Paschon[2], Edward J. Rebar[2], Frederic D. Bushman[3], Philip D. Gregory[2], Michael C. Holmes[2] & Katherine A. High[1,4]

Editing of the human genome to correct disease-causing mutations is a promising approach for the treatment of genetic disorders. Genome editing improves on simple gene-replacement strategies by effecting *in situ* correction of a mutant gene, thus restoring normal gene function under the control of endogenous regulatory elements and reducing risks associated with random insertion into the genome. Gene-specific targeting has historically been limited to mouse embryonic stem cells. The development of zinc finger nucleases (ZFNs) has permitted efficient genome editing in transformed and primary cells that were previously thought to be intractable to such genetic manipulation[1]. *In vitro*, ZFNs have been shown to promote efficient genome editing via homology-directed repair by inducing a site-specific double-strand break (DSB) at a target locus[2–4], but it is unclear whether ZFNs can induce DSBs and stimulate genome editing at a clinically meaningful level *in vivo*. Here we show that ZFNs are able to induce DSBs efficiently when delivered directly to mouse liver and that, when co-delivered with an appropriately designed gene-targeting vector, they can stimulate gene replacement through both homology-directed and homology-independent targeted gene insertion at the ZFN-specified locus. The level of gene targeting achieved was sufficient to correct the prolonged clotting times in a mouse model of haemophilia B, and remained persistent after induced liver regeneration. Thus, ZFN-driven gene correction can be achieved *in vivo*, raising the possibility of genome editing as a viable strategy for the treatment of genetic disease.

Viral-vector-mediated transfer of the wild-type copy of a gene that is defective in disease (gene replacement therapy) has been performed successfully in a variety of animal models and in humans[5–9]. However, disadvantages of gene replacement include risks related to insertional mutagenesis[10–12] and loss of endogenous regulatory signals that control gene expression. Gene-specific targeting in mouse induced pluripotent stem cells has highlighted the potential to overcome these challenges through *ex vivo* correction of a disease-causing mutation[13]. However, most genetic diseases affect organ systems in which *ex vivo* manipulation of target cells is not feasible. One such organ is the liver, the major site of synthesis of plasma proteins, including blood coagulation factors. A model genetic disease for gene therapy in the liver is haemophilia B, which is caused by deficiency of blood coagulation factor IX, encoded by the *F9* gene. Most affected individuals have circulating levels of factor IX that are below 1% of normal (5,000 ng ml^{-1}), but restoration to about 5% activity (250 ng ml^{-1}) converts severe haemophilia B to a mild form[14]. Most mutations in the *F9* gene are distributed across the coding sequences of exons 2–8 (Fig. 1a)[15]. Thus, specific targeting of any single mutant allele would not allow complete coverage of the wide spectrum of mutations found in the human population. However, ZFN-mediated targeting of a promoterless therapeutic gene fragment[2,16] (that is, a partial cDNA preceded by a splice acceptor site) into the first intron of *F9* would allow for splicing of a wild-type coding sequence with exon 1, leading to expression of functionally active factor IX and rescue of the defect caused by most mutations. We therefore sought to investigate whether ZFNs combined with a targeting vector carrying the wild-type *F9* exons 2–8 could induce gene targeting *in vivo* and correct a mutated *F9* gene *in situ*.

We designed ZFNs targeting intron 1 of the human *F9* (h*F9*) gene (F9 ZFNs, Supplementary Fig. 1) and confirmed their capacity to introduce a DSB at the intended target site (Fig. 1b) and to stimulate genome editing by homology-directed repair (HDR) in human erythroleukaemia K-562 cells (Fig. 1c, d). This ZFN pair was highly

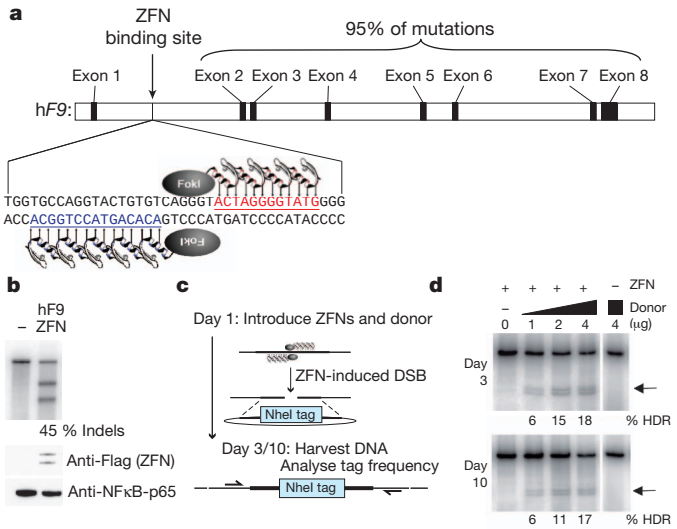

Figure 1 | F9 ZFNs cleave human *F9* intron 1 and induce homology-directed repair *in vitro*. **a**, F9 ZFNs target intron 1 of the human *F9* gene, allowing homology-directed repair upstream of 95% of *F9* mutations. **b**, K-562 cells were transfected with ZFN expression constructs (400 ng, right lane) or not transfected (left lane) and genomic DNA was harvested 3 d after transfection. The Cel-I assay was used to determine the frequency of ZFN-induced indels in both samples, indicated as '% Indels' below the right lane. Expression of Flag-tagged ZFN is confirmed by anti-Flag immunoblotting and anti-NFκB-p65 serves as a loading control. **c**, Schematic of RFLP assay, detailing ZFN-mediated targeting of a NheI restriction-site tag to the human *F9* gene. **d**, Co-transfection of 400 ng of ZFN expression plasmid with increasing amounts of NheI donor plasmid (0–4 μg) results in increasing levels of HDR at day 3 and day 10 after transfection, whereas transfection of the NheI donor alone (4 μg) does not result in detectable HDR. Black arrows denote NheI-sensitive cleavage products resulting from HDR. PCR was performed using ^{32}P-labelled nucleotides, followed by polyacrylamide gel electrophoresis (PAGE) and band-intensity quantification by autoradiography. Lanes with no quantification had no detectable HDR.

[1]Division of Hematology, CTRB 5000, Children's Hospital of Philadelphia, 3501 Civic Center Boulevard, Philadelphia, Pennsylvania 19104, USA. [2]Sangamo BioSciences, Point Richmond Tech Center, 501 Canal Boulevard, Suite A100, Richmond, California 94804, USA. [3]Department of Microbiology, 426 Johnson Pavilion, University of Pennsylvania School of Medicine, 3610 Hamilton Walk, Philadelphia, Pennsylvania 19104, USA. [4]Howard Hughes Medical Institute, 415 Curie Boulevard, Philadelphia, Pennsylvania 19104, USA.

active, driving small insertions and/or deletions (indels), characteristic of DSB repair by non-homologous end-joining (NHEJ), in up to 45% of alleles, and stable integration of the NheI restriction site in ~17–18% of alleles. This latter event is diagnostic of repair by HDR, using a homologous donor template designed to insert a novel restriction enzyme site into the *F9* locus. Similar results were obtained in the Hep3B human hepatocyte line (Supplementary Fig. 2). For *in vivo* evaluation, we generated a humanized mouse model of haemophilia B because the F9 ZFNs target a site in intron 1 of h*F9* that is absent from the murine gene. We constructed an h*F9* mini-gene[17], under the control of a liver-specific enhancer and promoter[18], that mimics a previously identified mutation (Y155stop)[19], resulting in the absence of circulating factor IX protein. We knocked in this mini-gene at the mouse ROSA26 locus[20], confirmed its genotype (Fig. 2a) and showed that the resulting transgenic mice had no detectable circulating human factor IX (Fig. 2b). We then crossed these mice (hereafter referred to as h*F9*mut mice) with an existing mouse model that has a deletion of the murine *F9* gene[21], generating h*F9*mut/HB mice to test ZFN-driven gene correction activity *in vivo* (Fig. 3a).

To deliver the F9 ZFNs to the liver, we generated a hepatotropic adeno-associated virus vector, serotype 8 (AAV8-ZFN) expressing the F9 ZFNs from a liver-specific enhancer and promoter[18]. To test the cleavage activity of the F9 ZFNs *in vivo*, we injected h*F9*mut mice through the tail vein with AAV8-ZFN and isolated liver DNA at day 7 after injection. Cleavage activity was measured via the surveyor nuclease

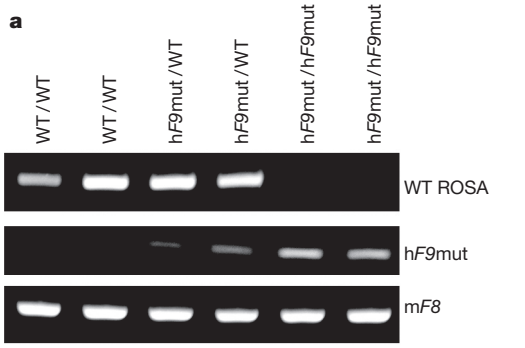

b

	WT / WT	h*F9*mut / h*F9*mut	h*F9*mut / h*F9*mut + AAV-hF.IX
Plasma hF.IX ng ml^{-1}	ND	ND	224

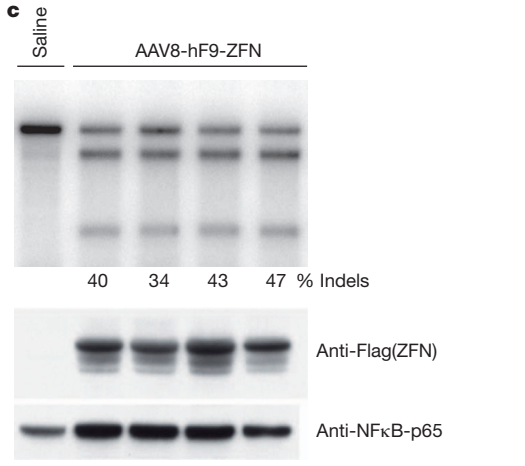

Figure 2 | AAV8-mediated delivery of F9 ZFNs to h*F9*mut mouse liver results in cleavage of h*F9*mut intron 1 *in vivo*. **a**, PCR genotyping of the parental strain (WT), a mouse heterozygous for the h*F9* mutant construct knocked into the ROSA26 locus (hF9mut/WT), and a mouse homozygous for h*F9*mut knocked into the ROSA26 locus (h*F9*mut/h*F9*mut). The murine factor VIII (m*F8*) PCR product indicates no inhibition of PCR. **b**, Human factor IX (hF.IX) levels in plasma, assayed by human factor IX ELISA, in wild-type mice, homozygous h*F9*mut mice and h*F9*mut mice injected with a viral vector expressing human factor IX (1×10^9 vector genomes (v.g.) AAV-human factor IX[20], injected via the tail vein). ND, none detected. **c**, Tail-vein injection of 1×10^{11} v.g. AAV8-ZFN expression vector into h*F9*mut mice results in cleavage of intron 1. The Cel-I assay was performed on liver DNA, isolated at day 7 after injection, to determine the frequency of ZFN-induced indels, indicated as '% Indels' below each lane, resulting from cleavage of the h*F9*mut intron. Lane with no quantification had no detectable cleavage products. Each lane represents an individual mouse. Expression of Flag-tagged ZFN was confirmed by anti-Flag immunoblotting of whole-liver lysate.

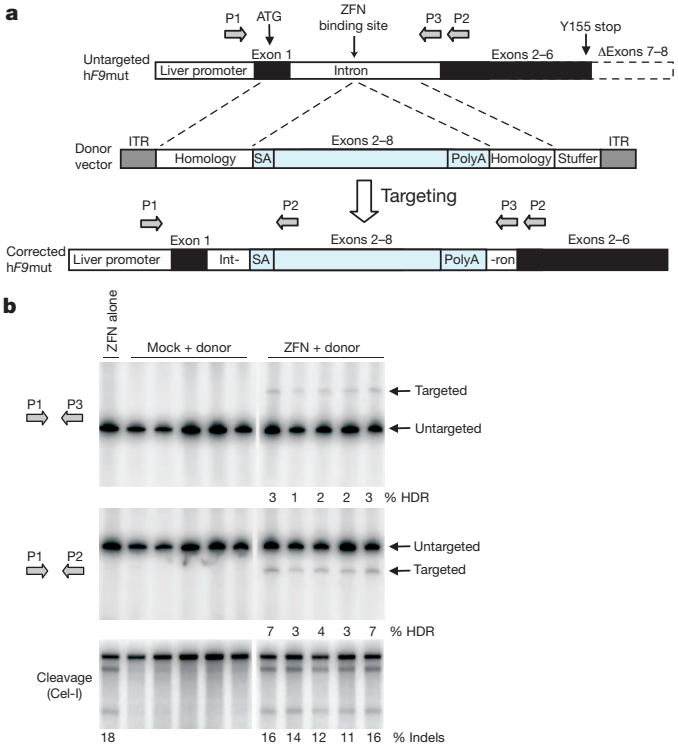

Figure 3 | F9 ZFNs promote AAV-mediated targeting of wild-type *F9* exons 2–8 to h*F9*mut intron 1 *in vivo*. **a**, The h*F9*mut gene mutation (truncation of exons 7 and 8) can be bypassed by targeted integration of h*F9* exons 2–8 into intron 1. Targeted and untargeted h*F9*mut alleles can be differentiated by PCR using primers P1, P2 and P3. The locations of the start codon and premature stop mutation are indicated by arrows. The left arm of homology spans from the beginning of exon 1 to the ZFN target site. (Deletion of exon 1 from the left homology arm does not alter results, see Supplementary Fig. 13.) The right arm of homology spans intronic sequence 3′ of the ZFN target site. polyA, polyadenylation site; SA, splice acceptor site. **b**, PCR analysis with primer pairs P1/P3 (upper panel) and P1/P2 (middle panel), showing successful gene targeting by HDR after intraperitoneal co-injection of 5×10^{10} v.g. AAV8-ZFN and 2.5×10^{11} v.g. AAV8-donor in h*F9*mut/HB mice at day 2 of life ($n=5$), but not after injection of 5×10^{10} v.g. AAV8-ZFN alone ($n=1$) or co-injection of 5×10^{10} v.g. AAV8-mock and 2.5×10^{11} v.g. AAV8-donor ($n=5$). The mock vector replaces F9 ZFN coding sequences with renilla luciferase. PCR was performed using ^{32}P-labelled nucleotides, followed by PAGE and quantification of product-band intensity by autoradiography to evaluate targeting frequency. Targeting frequencies are rounded down to the nearest whole number. Lower panel: intraperitoneal injection of AAV8-ZFN expression vector into h*F9*mut mice results in cleavage of intron 1. The Cel-I assay was performed on liver DNA to determine the frequency of ZFN-induced indels, indicated as '% Indels' below each lane, resulting from cleavage of the h*F9*mut intron. Lanes with no quantification had no detectable HDR or indels. Each lane represents an individual mouse.

(Cel-I) assay[22] which determines the frequency of indels that are characteristic of DSB repair by NHEJ. We observed mutation frequencies ranging from 34% to 47%, demonstrating that coupling of the F9 ZFNs with AAV8-mediated delivery promotes highly efficient genome modification in mouse liver (Fig. 2c). These results were confirmed by direct sequencing of the target locus (Supplementary Fig. 3).

To correct the mutated h*F9* gene *in situ*, we generated an AAV donor template vector (AAV8-donor) for gene targeting, with arms of homology flanking a corrective, partial cDNA cassette containing exons 2–8 of the wild-type h*F9* gene, flanked by splice-acceptor and poly-adenylation sites (Fig. 3a). Having established that we could detect HDR readily *in vitro* (Supplementary Fig. 4), we co-injected h*F9*mut/HB mice by intraperitoneal injection at day 2 of life with AAV8-ZFN + AAV8-donor, AAV8-mock + AAV8-donor or AAV8-ZFN alone. (Note that intraperitoneal injection in neonatal mice is less efficient than tail-vein injection in adult mice (compare Cel-I results in Fig. 3b to those in Fig. 2c) but it is used because it leads to higher survival rates.) At week 10 of life, we extracted liver DNA to assay gene replacement at the h*F9* locus via HDR. Using primers that hybridize to the chromosome outside the donor homology arms, generating a larger amplicon for a targeted allele (Fig. 3a, primers P1/P3 and Fig. 3b, upper panel), we observed HDR only in mice receiving both the donor and F9 ZFNs, with targeting efficiencies in the 1–3% range (Fig. 3b, upper panel). We confirmed HDR using alternative primers that hybridize to sites outside the donor homology arms and within the inserted cassette, respectively (Fig. 3a, primers P1/P2 and Fig. 3b, middle panel). Thus, co-delivery of ZFNs and a donor template, using AAV vectors, leads to HDR *in vivo*.

To determine whether ZFN-mediated gene targeting results in production of circulating human factor IX, we injected h*F9*mut mice intraperitoneally at day 2 of life with AAV8-ZFN alone, AAV8-mock + AAV8-donor or AAV8-ZFN + AAV8-donor. Human factor IX levels in the plasma of mice receiving ZFN alone or mock + donor averaged $<15\ \mathrm{ng\ ml^{-1}}$ (the lower limit of detection of the assay), whereas mice receiving ZFN + donor averaged 116–121 $\mathrm{ng\ ml^{-1}}$, corresponding to 2–3% of normal levels (Fig. 4a): significantly more than mice receiving ZFN alone and mice receiving mock + donor ($P \leq 0.006$ at all time points, 2-tailed *t*-test, Supplementary Fig. 5). Notably, in individual mice, the amount of circulating human factor IX correlated directly with the detected level of gene targeting via HDR (Supplementary Fig. 6).

To confirm stable genomic correction, we performed partial hepatectomies. Levels of human factor IX persisted after hepatectomies performed after genome editing (Fig. 4a), whereas an episomal AAV vector expressing human factor IX (AAV-human factor IX, Fig. 4b) showed markedly reduced human factor IX expression after hepatectomy, because extra-chromosomal episomes are lost during liver regeneration[23] (Fig. 4b). Control mice receiving ZFN alone or mock + donor continued to average $<15\ \mathrm{ng\ ml^{-1}}$ after hepatectomy (Fig. 4a) ($P \leq 0.01$ at all time points, 2-tailed *t*-test, Supplementary Fig. 5).

To ensure that the expression of human factor IX did not result from random donor integration into the genome, we injected wild-type mice (lacking the h*F9*mut mini-gene) intraperitoneally at day 2 of life with AAV8-ZFN alone, AAV8-mock + AAV8-donor or AAV8-ZFN + AAV8-donor. Notably, human factor IX levels in the plasma of mice in these groups averaged $<15\ \mathrm{ng\ ml^{-1}}$, $<30\ \mathrm{ng\ ml^{-1}}$ and $<30\ \mathrm{ng\ ml^{-1}}$, respectively (Fig. 4c), indicating that most of the expression of human factor IX in h*F9*mut mice treated with ZFN + donor came from specific gene correction. PCR targeting assays in these wild-type control mice were negative, indicating that amplicons used to quantify HDR were target-gene-specific (Supplementary Fig. 7).

To determine whether ZFN-mediated gene targeting would provide circulating levels of human factor IX that were sufficient to correct the haemophilia B phenotype, we injected h*F9*mut/HB mice intraperitoneally at day 2 of life with AAV8-ZFN alone, AAV8-mock + AAV8-donor or AAV8-ZFN + AAV8-donor. Levels of human factor IX in the plasma of mice receiving ZFN alone again averaged $<15\ \mathrm{ng\ ml^{-1}}$. Mice receiving mock + donor averaged $<25\ \mathrm{ng\ ml^{-1}}$ and mice receiving ZFN + donor had significantly higher levels of human factor IX ($P \leq 0.04$ at all time points compared to mock + donor, 2-tailed *t*-test, Supplementary Fig. 5), averaging 166–354 $\mathrm{ng\ ml^{-1}}$, 3–7% of normal circulating levels (Fig. 5a). A titration of AAV-donor showed that the

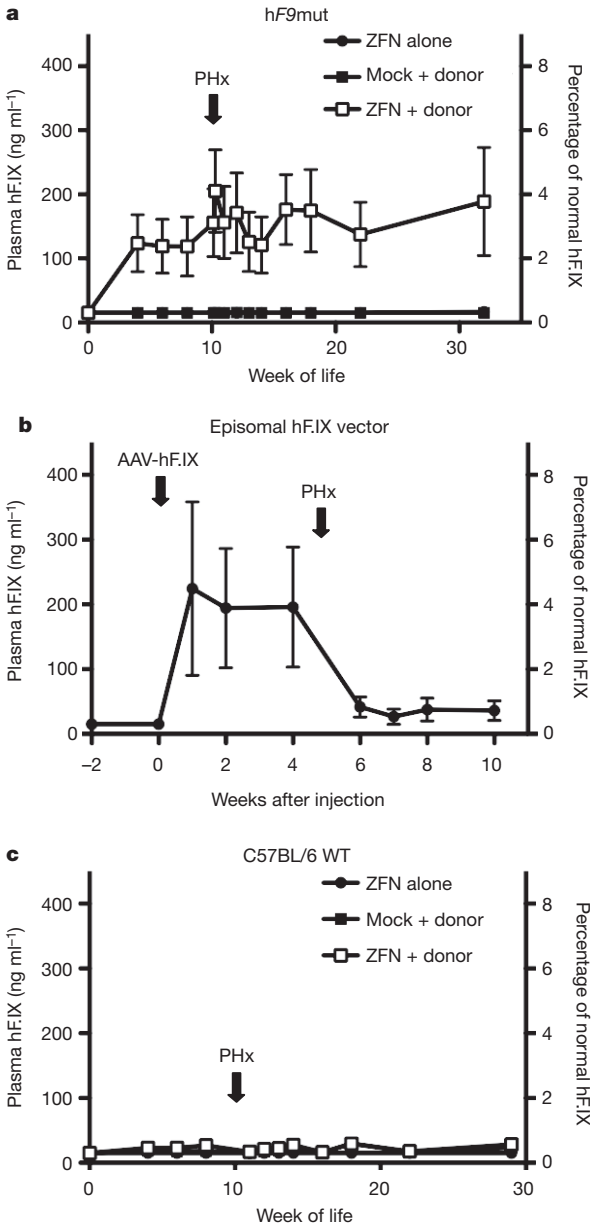

Figure 4 | *In vivo* h*F9*mut gene correction results in stable circulating factor IX. **a**, Levels of human factor IX in plasma of h*F9*mut mice after intraperitoneal injection at day 2 of life with either 5×10^{10} v.g. AAV8-ZFN alone ($n = 7$), 5×10^{10} v.g. AAV8-ZFN and 2.5×10^{11} v.g. AAV8-donor ($n = 7$), or 5×10^{10} v.g. AAV8-mock and 2.5×10^{11} v.g. AAV8-donor ($n = 6$). Partial hepatectomy (PHx) was performed at the time indicated by the arrow. Plasma levels of human factor IX were assayed by ELISA. Error bars denote s.e.m. **b**, Levels of human factor IX in plasma of wild-type mice ($n = 3$) after tail-vein injection of 1×10^{9} v.g. AAV-human-factor-IX (predominantly episomal), with subsequent PHx. Plasma levels of human factor IX were assayed by ELISA. Error bars denote s.e.m. **c**, Levels of human factor IX in plasma of wild-type C57BL/6J mice after intraperitoneal injection at day 2 of life with either 5×10^{10} v.g. AAV8-ZFN alone ($n = 8$ before PHx, $n = 4$ after PHx), 5×10^{10} v.g. AAV8-ZFN and 2.5×10^{11} v.g. AAV8-donor ($n = 9$ before PHx, $n = 5$ after PHx), or 5×10^{10} v.g. AAV8-mock and 2.5×10^{11} v.g. AAV8-donor ($n = 6$ before PHx, $n = 5$ after PHx). Plasma levels of human factor IX were assayed by ELISA. Error bars denote s.e.m.

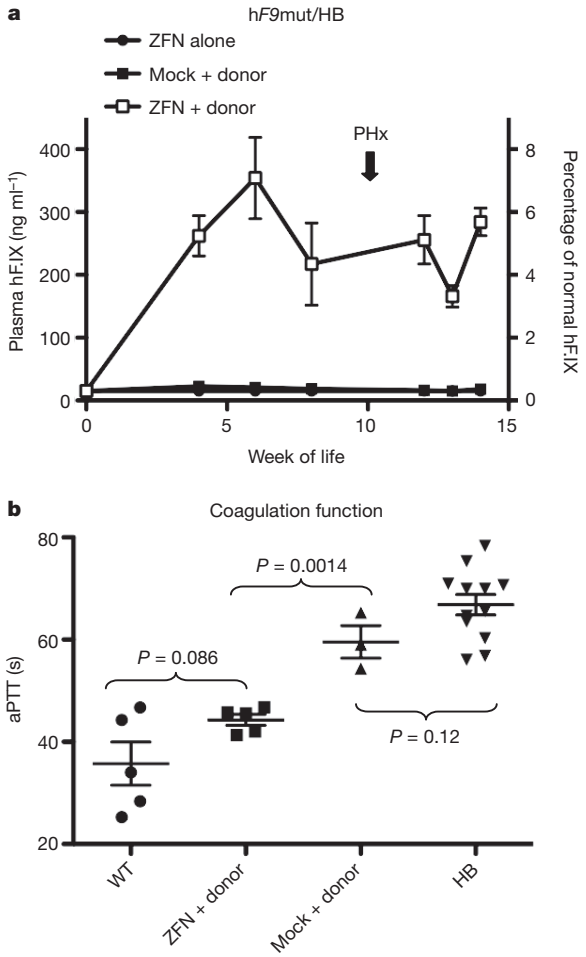

Figure 5 | Hepatic h*F9*mut gene correction results in phenotypic correction of haemophilia B. a, Levels of human factor IX in plasma of h*F9*mut/HB mice after intraperitoneal injection at day 2 of life with either 5×10^{10} v.g. AAV8-ZFN alone ($n = 10$ before PHx, $n = 1$ after PHx), 5×10^{10} v.g. AAV8-ZFN and 2.5×10^{11} v.g. AAV8-donor ($n = 9$ before PHx, $n = 5$ after PHx), or 5×10^{10} v.g. AAV8-mock and 2.5×10^{11} v.g. AAV8-donor ($n = 9$ before PHx, $n = 3$ after PHx). Plasma levels of human factor IX were assayed by ELISA. Error bars denote s.e.m. **b**, Test of clot formation by aPTT at week 14 of life in mice that had received intraperitoneal injection at day 2 of life with 5×10^{10} v.g. AAV8-ZFN and 2.5×10^{11} v.g. AAV8-donor ($n = 5$) or 5×10^{10} v.g. AAV8-mock and 2.5×10^{11} v.g. AAV8-donor ($n = 3$). The aPTTs of wild-type (WT, $n = 5$) and haemophilia B (HB, $n = 12$) mice are shown for comparison. *P*-values are from 2-tailed Student's *t*-test of WT versus ZFN + donor, ZFN + donor versus mock + donor and mock + donor versus HB. Error bars denote s.e.m.

degree of correction was dependent on the dose of AAV-donor (Supplementary Fig. 8). To determine whether the haemophilia B phenotype was corrected, we assayed activated partial thromboplastin time (aPTT), a measure of clot-formation kinetics that is markedly prolonged in haemophilia. The average aPTTs for wild-type mice ($n = 5$) and haemophilia B mice ($n = 12$) were 36 s and 67 s, respectively (Fig. 5b). Mice receiving mock + donor ($n = 3$) averaged 60 s, whereas mice receiving ZFN + donor ($n = 5$) had significantly shortened aPTTs, averaging 44 s ($P = 0.0014$ compared to mock + donor, 2-tailed *t*-test). Clotting times for ZFN + donor and wild-type mice were not significantly different ($P = 0.086$, 2-tailed *t*-test, Fig. 5b). Together, these data demonstrate a clinically significant correction of the coagulation defect in haemophilia B, via direct *in vivo* delivery of ZFNs to mediate permanent correction of the genome in mouse hepatocytes.

To begin to evaluate the specificity of this approach, we used a method based on the systematic evolution of ligands by exponential enrichment (SELEX)[22] to identify the top 20 potential off-target sites for the F9 ZFNs in the mouse genome. Cel-I assays performed at each of these sites were unable to detect cleavage in 19 out of 20 (lower limit of detection 1%). At the twentieth site, located in an intergenic region at mouse chromosome 9qE3.1, we detected cleavage at a tenth the frequency seen at the *F9* target site (Supplementary Fig. 9). Thus, the specificity of the hF9 ZFNs is comparable to CCR5-specific ZFNs, by this analysis[22].

To investigate the specificity of the ZFN approach further, we used ligation-mediated PCR and 454 pyrosequencing to detect sites of AAV vector integration genome-wide[24]. A comparison of ZFN + donor and mock + donor mice revealed similar distributions of AAV integration sites across the mouse genome (Supplementary Fig. 10); this integration site distribution was consistent with previously reported data showing that genes[24,25], but not oncogenes, were favoured as integration sites. We next validated the prediction from *in vitro* studies[26] that a ZFN-induced DSB would capture the AAV vector itself, by employing a direct PCR approach using primers that anneal to the h*F9*mut locus and the AAV inverted terminal repeat (ITR) (Supplementary Fig. 11). This assay confirmed AAV integration at the ZFN target site in ZFN + donor mice but not in mock + donor mice. Finally, a pre-clinical evaluation of toxicity in injected and control mice showed no effects on growth or weight gain in either h*F9*mut or wild-type mice ($n = 43$) over 8 months of observation (data not shown), and no changes in liver function tests at 4, 29 and 32 weeks after injection (Supplementary Fig. 12), indicating that the treatment was well tolerated.

Studies showing that ZFNs can mediate gene correction efficiently through the introduction of site-specific DSBs, and can induce HDR in cultured cells, have provided important proof-of-concept results for the clinical application of engineered nucleases for diseases affecting cells that can be removed and returned to the patient. However, the necessity to isolate and manipulate cells *ex vivo* limits the application of this technology to a subset of genetic diseases. Our results show that AAV-mediated delivery of a donor template and ZFNs *in vivo* induces gene targeting, resulting in measurable circulating levels of factor IX. This therapeutic strategy is sufficient to restore haemostasis in a mouse model of haemophilia B, thus demonstrating genome editing in an animal model of a disease. Clinical translation of these results will require optimization of correction efficiency and a thorough analysis of off-target effects in the human genome, an issue that we have begun to monitor. Together, these data show that AAV-mediated delivery of ZFNs and a donor template gives rise to persistent and clinically meaningful levels of genome editing *in vivo*, and thus can be an effective strategy for targeted gene disruption or *in situ* correction of genetic disease *in vivo*.

METHODS SUMMARY

Zinc finger nucleases targeting the h*F9* gene were designed and validated as described in Methods. ZFN expression, donor template and AAV-vector-production plasmids were constructed using standard molecular biology techniques. AAV vectors were produced through triple transfection of HEK 293T cells. K-562, Hep3B and HEK 293T cells were cultured and transfected using standard techniques. h*F9*mut mice were created by targeted transgenesis as described in Methods. Mouse injections, plasma collection and surgical procedures were approved by the Children's Hospital of Philadelphia institutional animal care and use committee, and performed as described in Methods. The Cel-I assay, target-site sequencing, restriction-fragment length polymorphism (RFLP) knock-in assay, targeting assay, human factor IX enzyme-linked immunosorbent assay (ELISA), aPTT, liver function tests, SELEX, ligation-mediated PCR and 454 sequencing were all performed as described in Methods.

Full Methods and any associated references are available in the online version of the paper at www.nature.com/nature.

Received 29 October 2010; accepted 6 May 2011.
Published online 26 June 2011.

1. Urnov, F. D., Rebar, E. J., Holmes, M. C., Zhang, H. S. & Gregory, P. D. Genome editing with engineered zinc finger nucleases. *Nature Rev. Genet.* **11,** 636–646 (2010).

2. Urnov, F. D. *et al.* Highly efficient endogenous human gene correction using designed zinc-finger nucleases. *Nature* **435,** 646–651 (2005).
3. Porteus, M. H. & Baltimore, D. Chimeric nucleases stimulate gene targeting in human cells. *Science* **300,** 763 (2003).
4. Bibikova, M. *et al.* Stimulation of homologous recombination through targeted cleavage by chimeric nucleases. *Mol. Cell. Biol.* **21,** 289–297 (2001).
5. Cartier, N. *et al.* Hematopoietic stem cell gene therapy with a lentiviral vector in X-linked adrenoleukodystrophy. *Science* **326,** 818–823 (2009).
6. Aiuti, A. *et al.* Gene therapy for immunodeficiency due to adenosine deaminase deficiency. *N. Engl. J. Med.* **360,** 447–458 (2009).
7. Cideciyan, A. V. *et al.* Human gene therapy for RPE65 isomerase deficiency activates the retinoid cycle of vision but with slow rod kinetics. *Proc. Natl Acad. Sci. USA* **105,** 15112–15117 (2008).
8. Maguire, A. M. *et al.* Safety and efficacy of gene transfer for Leber's congenital amaurosis. *N. Engl. J. Med.* **358,** 2240–2248 (2008).
9. Bainbridge, J. W. *et al.* Effect of gene therapy on visual function in Leber's congenital amaurosis. *N. Engl. J. Med.* **358,** 2231–2239 (2008).
10. Cavazzana-Calvo, M. *et al.* Transfusion independence and *HMGA2* activation after gene therapy of human β-thalassaemia. *Nature* **467,** 318–322 (2010).
11. Howe, S. J. *et al.* Insertional mutagenesis combined with acquired somatic mutations causes leukemogenesis following gene therapy of SCID-X1 patients. *J. Clin. Invest.* **118,** 3143–3150 (2008).
12. Hacein-Bey-Abina, S. *et al. LMO2*-associated clonal T cell proliferation in two patients after gene therapy for SCID-X1. *Science* **302,** 415–419 (2003).
13. Hanna, J. *et al.* Treatment of sickle cell anemia mouse model with iPS cells generated from autologous skin. *Science* **318,** 1920–1923 (2007).
14. Pollak, E. S. & High, K. A. in *The Metabolic and Molecular Bases of Inherited Disease* (eds Scriver, C. R., Beaudet, A. L., Valle, D. & Sly, W. S.) 4393–4413 (McGraw-Hill, 2001).
15. Green, P. *Haemophilia B Mutation Database* ⟨http://www.kcl.ac.uk/ip/petergreen/haemBdatabase.html⟩ (2004).
16. Moehle, E. A. *et al.* Targeted gene addition into a specified location in the human genome using designed zinc finger nucleases. *Proc. Natl Acad. Sci. USA* **104,** 3055–3060 (2007).
17. Manno, C. S. *et al.* Successful transduction of liver in hemophilia by AAV-Factor IX and limitations imposed by the host immune response. *Nature Med.* **12,** 342–347 (2006).
18. Miao, C. H. *et al.* Inclusion of the hepatic locus control region, an intron, and untranslated region increases and stabilizes hepatic factor IX gene expression *in vivo* but not *in vitro. Mol. Ther.* **1,** 522–532 (2000).
19. Thompson, A. R. & Chen, S. H. Germ line origins of de novo mutations in hemophilia B families. *Hum. Genet.* **94,** 299–302 (1994).
20. Zambrowicz, B. P. *et al.* Disruption of overlapping transcripts in the ROSA βgeo 26 gene trap strain leads to widespread expression of β-galactosidase in mouse embryos and hematopoietic cells. *Proc. Natl Acad. Sci. USA* **94,** 3789–3794 (1997).
21. Lin, H. F., Maeda, N., Smithies, O., Straight, D. L. & Stafford, D. W. A coagulation factor IX-deficient mouse model for human hemophilia B. *Blood* **90,** 3962–3966 (1997).
22. Perez, E. E. *et al.* Establishment of HIV-1 resistance in CD4+ T cells by genome editing using zinc-finger nucleases. *Nature Biotechnol.* **26,** 808–816 (2008).
23. Nakai, H. *et al.* Extrachromosomal recombinant adeno-associated virus vector genomes are primarily responsible for stable liver transduction *in vivo. J. Virol.* **75,** 6969–6976 (2001).
24. Li, H. *et al.* Assessing the potential for AAV vector genotoxicity in a murine model. *Blood* **117,** 3311–3319 (2011).
25. Nakai, H. *et al.* AAV serotype 2 vectors preferentially integrate into active genes in mice. *Nature Genet.* **34,** 297–302 (2003).
26. Miller, D. G., Petek, L. M. & Russell, D. W. Adeno-associated virus vectors integrate at chromosome breakage sites. *Nature Genet.* **36,** 767–773 (2004).

Supplementary Information is linked to the online version of the paper at www.nature.com/nature.

Acknowledgements This work was funded by the National Institutes of Health and the Howard Hughes Medical Institute.

Author Contributions H.L., V.H., Y.D., T.L., S.L.M., P.D.G., M.C.H. and K.A.H. designed the experiments. H.L., V.H., Y.D., T.L., S.Y.W., A.S.B., N.M., X.M.A., R.S., L.I., S.L.M., J.D.F., F.R.K., S.Z., D.E.P. and E.J.R. generated reagents and performed the experiments. H.L., Y.D., F.D.B., P.D.G., M.C.H. and K.A.H. wrote and edited the manuscript.

Author Information Reprints and permissions information is available at www.nature.com/reprints. The authors declare competing financial interests: details accompany the full-text HTML version of the paper at www.nature.com/nature. Readers are welcome to comment on the online version of this article at www.nature.com/nature. Correspondence and requests for materials should be addressed to K.A.H. (high@email.chop.edu) or M.C.H. (mholmes@sangamo.com; requests for zinc-finger nuclease reagents described in the paper).

METHODS

ZFN reagents. ZFNs targeting the h*F9* gene were designed by modular assembly using an archive of zinc finger proteins, as previously described[2]. The full amino acid sequences of the F9 ZFN pair are in Supplementary Fig. 1. The ZFN expression vector that was used *in vitro* was assembled as previously described[27]. The F9 ZFN AAV production plasmid was constructed by transferring the coding sequence into pRS115, a vector containing the AAV2 ITRs. ZFN expression was under the control of the ApoE enhancer and hα_1AT promoter from the previously described pAAV-hFIX16 plasmid[17].

Targeting vectors. The NheI RFLP donor plasmid was constructed by amplifying 1-kb regions flanking the ZFN cleavage site from K-562-cell genomic DNA. A short sequence containing the NheI restriction site was subsequently introduced between the left and right arms of homology, as described in ref. 16. The NotI RFLP donor plasmid was constructed by amplifying the left (1 kb) and right (0.6 kb) arms of homology flanking the ZFN cleavage site from h*F9*mut mouse genomic DNA and cloning these into the production plasmid that contains the AAV2 ITRs, pRS165. A short sequence containing the NotI restriction site was subsequently introduced between the left and right arms of homology, as previously described[16]. The targeting vector used *in vivo* was built by cloning a cassette containing the splice acceptor, the coding sequence of exons 2–8 and the bovine growth hormone polyA signal from the pAAV-hFIX16 plasmid[20] into the NotI RFLP donor plasmid.

Cell culture and transfection. K-562 cells (ATCC) were maintained at 37 °C under 5% CO_2 in RPMI medium supplemented with 10% FBS, and were transfected using the 96-well Nucleofector kit SF (Lonza) as per the manufacturer's recommendations. Hep3B cells (ATCC) were maintained at 37 °C under 5% CO_2 in DMEM medium supplemented with 10% FBS, and were transfected using the 96-well Nucleofector kit SE (Lonza). HEK 293T cells (ATCC) were maintained at 37 °C under 5% CO_2 in DMEM medium supplemented with 10% FBS, and were transfected using the 96-well Nucleofector kit SF (Lonza). Lentiviral vector for stable transduction of the h*F9*mut mini-gene into HEK 293T cells was made using the ViraPower HiPerform lentiviral expression system (Invitrogen).

Surveyor nuclease (Cel-I) assay and target-site sequencing. Genomic DNA from K-562 and Hep3B cells was extracted using the QuickExtract DNA extraction solution (Epicentre Biotechnologies). ZFN target loci were amplified by PCR (30 cycles, 60 °C annealing and 30 s elongation at 68 °C) using the hF9cel1 forward primer (TCGGTGAGTGATTTGCTGAG) and hF9cel1 reverse primer (AACCT CTCACCTGGCCTCAT). Genomic DNA from mouse liver was isolated using the MasterPure complete DNA purification kit (Epicentre Biotechnologies). Primers for Cel-I of the h*F9*mut construct were hF9mut-cel1 forward (CTAGTAGCT GACAGTACC) and hF9mut-cel1 reverse (GAAGAACAGAAGCCTAATTA TG). The locus was amplified for 30 cycles (50 °C annealing and 30 s elongation at 68 °C). The assays were carried out as described previously[22]. For target-site sequencing, amplicons were cloned into the pCR-TOPO vector (Invitrogen) and sequenced using the primers M13forward (GTAAAACGACGGCCAGTG) and M13reverse (GGAAACAGCTATGACCATG).

RFLP knock-in and targeting assays. Genomic DNA was extracted from K-562 and Hep3B cells using QuickExtract DNA extraction solution (Epicentre Biotechnologies). Genomic DNA from mouse liver was isolated using the MasterPure complete DNA purification kit (Epicentre Biotechnologies). The h*F9* locus was amplified by 25 cycles of PCR (3 min extension at 68 °C and 30 s annealing at 55 °C) in the presence of radiolabelled dNTPs, using the hF9-TI forward (GGCCTTATTTACACAAAAAGTCTG) and hF9-TI reverse (TTTGC TCTAACTCCTGTTATCCATC) primers. The PCR products were then purified with G50 columns, digested with NheI, resolved by 5% PAGE and autoradiographed. RFLP assays in HEK 293T cells transduced with the h*F9*mut mini-gene were genotyped as described above, using the P1 (ACGGTATCGATAAG CTTGATATCGAATTCTAG) and P2 (CACTGATCTCCATCAACATACTGC) primers, and the PCR products (25 cycles, 63 °C annealing and 2 min extension at 65 °C) were digested with NotI. To quantify the targeting of the 'splice acceptor – exons 2–8 coding sequence – bovine growth hormone polyA signal' cassette, gDNA was amplified using the P1 and P3 (GAATAATTCTTTAGTTTTA GCAA) or the P1 and P2 primer pairs by 25 cycles of PCR (4 min extension time at 65 °C and 30 s annealing at 48 °C) in the presence of radiolabelled dNTPs. The PCR products were then purified with G50 columns, resolved by 5% PAGE and autoradiographed. All PCR reactions were performed using Accuprime Taq HiFi (Invitrogen). To capture the NHEJ-mediated insertion of the AAV vector at the h*F9* ZFN cut-site, gDNA was amplified using P1 and P4 (AGGAACC CCTAGTGATGGAG) primers by 25 cycles of PCR (80 s extension time at 65 °C) in the presence of radiolabelled dNTPs. The PCR reactions were performed using Phusion High-fidelity DNA polymerase (New England BioLabs) in conjunction with GC Buffer and 3% dimethylsulphoxide. The PCR products were then purified with G50 columns, resolved by 5% PAGE and autoradiographed.

h*F9*mut mouse generation. The h*F9*mut construct (sequence provided in Supplementary Fig. 14) was constructed by gene synthesis (Genscript) and ligated into the pUC57 plasmid. The h*F9*mut construct was then excised and ligated into a proprietary plasmid between FLP recombinase sites compatible for recombinase-mediated cassette exchange (RCME) (Taconic-Artemis), to create the h*F9*mut KI plasmid. The h*F9*mut KI plasmid and a FLP recombinase expression plasmid (Taconic-Artemis) were transfected into B6S6F1 embryonic stem (ES) cells (Taconic-Artemis) containing FLP recombinase sites compatible for RCME at the ROSA26 locus[20]. Correctly targeted B6S6F1-h*F9*mut ES cell clones were identified by Southern blot and injected into B6D2F1 blastocysts. Pure ES-cell-derived B6S6F1-h*F9*mut mice (G0) were delivered by natural birth and chimaeric pups were backcrossed with C57BL/6J mice (Jackson Laboratories) for 5 generations (for *in vivo* cleavage experiments) or 7–10 generations (for *in vivo* gene targeting experiments). h*F9*mut mice were genotyped using primers h*F9*mut Oligo 1 (ACTGTCCTCTCATGCGTTGG), h*F9*mut Oligo 2 (GATGTTGGAGGTGGCA TGG), wtROSA Oligo 1 (CATGTCTTTAATCTACCTCGATGG), wtROSA Oligo 2 (CTCCCTCGTGATCTGCAACTCC), mFVIII Oligo1 (GAGCAAATTC CTGTACTGAC) and mFVIII Oligo 2 (TGCAAGGCCTGGGCTTATTT). HB mice have been backcrossed with C57BL/6J mice (Jackson Laboratories) for >10 generations and were genotyped using previously described primers[20]. C57BL/6J mice (Jackson Laboratories) were used for h*F9*mut-negative gene targeting experiments.

AAV vector production. AAV serotype 8 vectors were produced by triple transfection methods into HEK 293T cells, and subsequent CsCl density-gradient purification, as previously described[28].

Animal experiments. AAV vector was diluted to 200 µl with PBS before tail-vein injection. AAV vector was diluted to 20 µl with PBS before neonatal intraperitoneal injection. Plasma for human factor IX ELISA was obtained by retro-orbital bleeding into heparinized capillary tubes. Plasma for aPTT was obtained by tail bleeding, 9:1 into 3.8% sodium citrate. Partial hepatectomies were performed as previously described[29]. Tissue for nucleic acid analysis was immediately frozen on dry ice after necropsy. All animal procedures were approved by the institutional animal care and use committee of the Children's Hospital of Philadelphia.

SELEX. *In silico* identification of potential off-target ZFN cleavage sites was performed by identifying homologous regions within the genome, as previously described[22].

LM-PCR and 454 sequencing. AAV-donor integration junctions were cloned and sequenced as previously described[24]. In brief, genomic DNA from mouse liver was isolated using the MasterPure complete DNA purification kit (Epicentre Biotechnologies). 1 µg of DNA was digested with MseI (New England Biolabs) and 1 µg of DNA was digested with CviQ1 (New England Biolabs) for 16 h at 37 °C. These two enzymes were chosen for their ideal proximity to the target site. Digested DNA was purified using a PCR purification kit (Qiagen), then a previously described double-stranded linker[24] was ligated to digested DNA ends using T4 DNA ligase (New England Biolabs) for 16 h at 16 °C. Integration junctions were then PCR-amplified using an adaptor primer (GTAATACGACTCACTATAG GGC) and a stuffer primer (CTCCAACTCCTAATCTCAGGTGATCTACCC). PCR products were diluted 1:200 in TE buffer and integration junctions were PCR-amplified again, using a second adaptor primer (CGTATCGCCTCCCTC GCGCCATCAGnnnnnnnnnnAGGGCTCCGCTTAAGGGAC, where nnnnnnnnnn is a sample-specific barcode) and a second stuffer primer (CTATGCGCCTTGCC AGCCCGCTCAGnnnnnnnnnnACCTTGGCCTCCCAAATTGCTGGG, where nnnnnnnnnn is a sample-specific barcode). Amplified integration junctions were then sequenced using a Genome Sequencer FLX pyrosequencer (Roche/454).

Integration-site analysis. Pyrosequencing reads were first decoded using DNA barcodes, separating sequence reads by mouse. Reads were then aligned against the linker and stuffer primers using the Crossmatch program (-minmatch 8 -penalty −2 -minscore 6). Reads matching one or the other primer were then aligned using BLAT against three target sequences: the stuffer, the AAV-ITR and the h*F9*mut construct. BLAT parameters were optimized to find repetitive and/or short-sequence hits against each target sequence (-stepSize = 3, -tileSize = 8, -repMatch = 16384, -minScore = 5, -minIdentity = 50, -oneOff = 1). Additionally, BLAT fastMap option was included for alignment against the stuffer and the h*F9*mut construct. BLAT hits originating from the ITR were processed as previously described[24]. BLAT hits originating from the stuffer and the h*F9*mut construct were identified by requiring a unique high-scoring match requiring at least 90% sequence identity with a ≤5-base-pair gap. All the BLAT hits from each of the three target sequences were consolidated and ordered by their location within each read. Reads that had stuffer and/or linker with ITR but no h*F9*mut construct were segregated and aligned using BLAT against the mouse genome. BLAT hits in the mouse genome were scored using the same criteria as described above and were required not to overlap with hits originating from stuffer, ITR and linker. A master table of all the reads and their respective target hits was constructed to manage the

alignment data and associated metadata. All the subsequent 454 analysis was carried out using this master table. Sequence analysis and control of mispriming was carried out separately for reads originating from each primer (stuffer or linker). To remove reads originating from mispriming at the stuffer primer, we required that each read involving the stuffer primer must extend through 30 base pairs (bp) of adjoining stuffer sequence and at least 13 bp of the flanking ITR. For reads originating on the linker side, we required that reads include at least 13 bp of ITR and at least 15 bases of the stuffer. Integration sites in the mouse genome were analysed as previously described[30].

Human factor IX quantification and functional analysis. Quantification of human factor IX in plasma was performed using a human factor IX ELISA kit (Affinity Biologicals), with a standard curve from pooled normal human plasma (Trinity Biotech). All readings below the last value of the standard curve (15 ng ml^{-1}) were arbitrarily given the value of 15 ng ml^{-1}, the limit of detection. The assay of activated partial thromboplastin time (aPTT) was performed by mixing sample plasma 1:1:1 with pooled haemophilia B human plasma (George King Biomedical, Inc.) and aPTT reagent (Trinity Biotech). Clot formation was initiated by addition of 25 mM calcium chloride.

Liver function tests. Quantification of plasma alanine aminotransferase (ALT) was performed using an ALT(SGPT) reagent set (Teco Diagnostics) colorimetric assay.

Statistics. Student's *t*-test was used as described. Linear regressions were performed using Prism (Graphpad). In all tests, differences were considered significant at $P < 0.05$.

27. Doyon, Y. *et al.* Heritable targeted gene disruption in zebrafish using designed zinc-finger nucleases. *Nature Biotechnol.* **26,** 702–708 (2008).
28. Ayuso, E. *et al.* High AAV vector purity results in serotype- and tissue-independent enhancement of transduction efficiency. *Gene Ther.* **17,** 503–510 (2010).
29. Mitchell, C. & Willenbring, H. A reproducible and well-tolerated method for 2/3 partial hepatectomy in mice. *Nature Protocols* **3,** 1167–1170 (2008).
30. Berry, C., Hannenhalli, S., Leipzig, J. & Bushman, F. D. Selection of target sites for mobile DNA integration in the human genome. *PLoS Comput. Biol.* **2,** e157 (2006).